Design of an Array Feed Offset Parabolic Reflector Antenna by Using Electromagnetic Simulations and Measured Results

N. Michishita[1], J. Shinohara[1], Y. Yamada[1], M. T. Islam[2], and N. Misran[2]

[1] National Defense Academy, 1-10-20 Hashirimizu, Yokosuka, Japan
yyamada@nda.ac.jp

[2] Universiti Kebangsaan Malaysia, 43600 Bangi, Selangor Darul Ehsan, Malaysia
tariqul@ukm.my

Abstract ─ Offset parabolic reflector antennas are well-known for their very simple configurations and are widely used. However, low antenna gain sometimes results in inconvenient operation. In order to increase the antenna gain, an array feed is generally employed to correct the antenna aperture distribution. However, accurate and low-loss realization methods for array feeds were not studied sufficiently. In this work, radiation pattern synthesis is first performed at the array feed to achieve uniform aperture distribution. As a result of this synthesis, the array excitation coefficients are determined. Further, accurate design methods for corporate feed line networks to obtain the required excitation coefficients and low feeder loss through electromagnetic simulations are described. Finally, the designed array feed is fabricated, and the measured radiation patterns are compared with the calculated results. Moreover, the array feed is combined with the fabricated offset reflector, and the antenna radiation patterns and gains are obtained. An increase in the antenna gain is ensured.

Index Terms – Array feed, electromagnetic simulation, offset parabolic reflector, and radiation pattern synthesis.

I. INTRODUCTION

Offset parabolic reflector antennas are well-known for their very simple configuration and ease of installation. Currently, these antennas are widely used as satellite broadcasting receivers [1] and vehicle mounted uses for satellite communications [2]. Previously, an important review of this type of antenna was reported [3], and an example of a shaped beam obtained by weighted array feeds [4] was cited. Recently, simple design formulas for linear array feeds were reported [5]. As for the array feeds, examples of the fabrication of a small-number array [6] and a large-number array [7] were reported. In the case of a small-number array, it was reported that the error in the corporate feed design and feeder loss results in 1 to 2 dB of array feed loss. For realizing appropriate and low-loss array feeds, accurate design of array excitations, arrangement of corporate feed lines, and accurate fabrication are required.

In this paper, an accurate and low-loss realization method for array feeds is described. First, the radiation pattern of an array feed is determined in order to increase the antenna gain of the offset reflector antenna. The excitation coefficients of the array elements are obtained through radiation pattern synthesis of the array feed in order to achieve uniform illumination of the offset antenna aperture. Further, corporate feed line network designs are performed by using a commercial electromagnetic simulator called FEKO. The main feature of the proposed feed line network is a coplanar feeder line arrangement for achieving a single feed point. Feed lines of appropriate lengths and power dividing ratios are designed on the basis of the accurate simulation results of the array excitations. In order to ensure design accuracies, an actual array feed is fabricated. Finally, the radiation patterns are

Submitted On: March 20, 2013
Accepted On: Jan. 1, 2014

measured by using a combination of the fabricated array feed and the offset reflector.

II. DESIGN OF AN ARRAY FEED

A. Array excitation coefficients for a shaped beam

The antenna configuration is shown in Fig. 1. The offset parabolic reflector is fed by an array feed. The antenna aperture illumination $E_a(\rho)$ is determined from the simple relation to the radiation pattern $E_f(\theta_f)$ of the array feed as follows,

$$E_a(\rho) = \frac{1}{2f} E_f(\theta_f) \cos^2(\theta/2) \cdot \quad (1)$$

For achieving uniform illumination on the aperture plane, $E_f(\theta_f)$ must satisfy the following expression,

$$E_f(\theta_f) = \frac{2f}{\cos^2(\theta/2)} . \quad (2)$$

The shape of $E_f(\theta_f)$ given by equation (2) is shown in Fig. 2. The strengths are normalized by the value at the angle θ_u. The required $E_f(\theta_f)$ has the shape of a slope. This shape is quite different from those of the ordinal radiators.

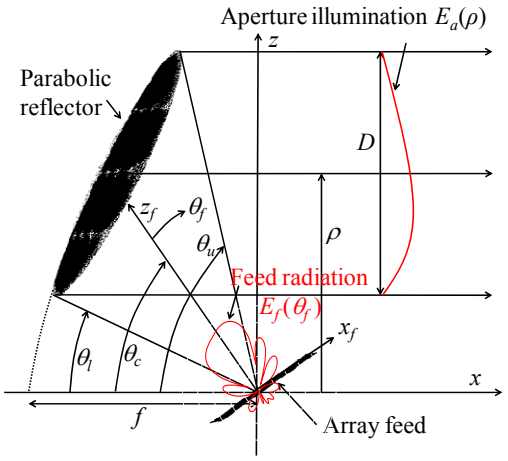

Fig. 1. Antenna configuration.

For achieving the radiation pattern in Fig. 2, the array feed configuration shown in Fig. 3 is used. A planar array configuration is employed. The array is composed of three column arrays and six row patches. Radiation pattern synthesis is performed in the column array, and $E_f(\theta_f)$ is achieved in the z_f-x_f plane. The three column arrays are used to form a radiation pattern in the z_f-y_f plane. The three column arrays have the same excitation values in order to adequately illuminate the reflector.

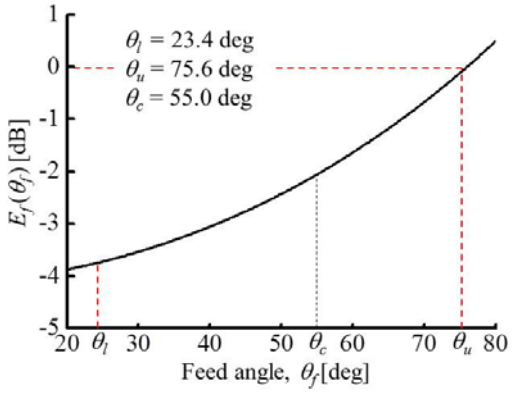

Fig. 2. Feed radiation pattern for achieving uniform $E_a(\rho)$.

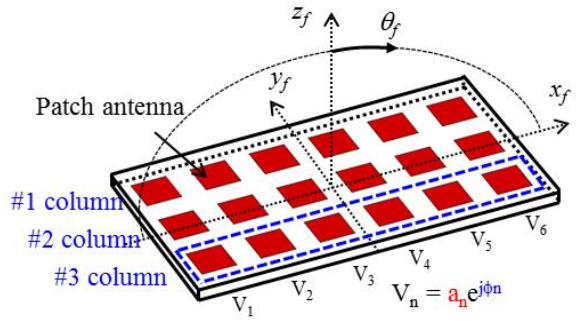

Fig. 3. Configuration of an array feed.

Radiation pattern synthesis is performed by determining the array excitation coefficients, which are denoted as $V_n = a_n e^{j\phi n}$. The excitation coefficients of the array elements are determined through the least mean square method [8]. The above calculation is performed using the following expression,

$$[V] = ([B]^H[T_0][B])^{-1}[B]^H[T_0][A] \quad (3)$$

where [V] is the excitation coefficient vector, and [A] is the radiation pattern vector that corresponds to the objective radiation pattern in Fig. 2. $[T_0]$ is a weighting matrix, which emphasizes the important direction in the radiation pattern, and [B] denotes the contributions of [V] to the array radiation pattern.

The synthesized radiation pattern ([F]) and [A] are shown in Fig. 4 (a). At [A], the reflector exists between angles θ_l and θ_u. Near the edges of the

reflector, the radiation levels are decreased by approximately -10 dB in order to suppress the spillover from the reflector. In all the radiation regions, [F] is well-designed with regard to [A]. The radiation pattern in the z_f-y_f plane is shown in Fig. 4 (b). At the reflector edges, the radiation levels are suppressed by approximately -10 dB.

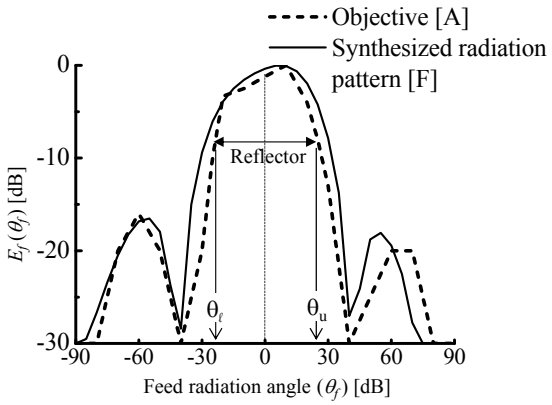

(a) Feed pattern for uniform $E_a(\rho)$.

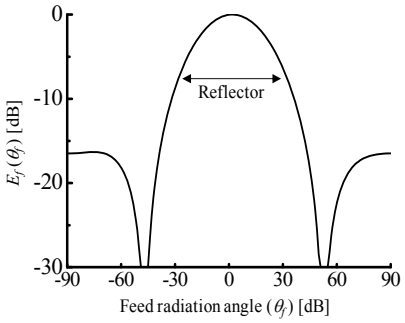

(b) Radiation pattern in the z_f-y_f plane.

Fig. 4. Feed radiation patterns.

The excitation coefficients designed using equation (3) are shown in Fig. 5. The amplitudes are symmetrical on both sides of the array. The phases are rotationally symmetrical around the center of the array. In the excitation phases, there are very steep changes at the two end elements. The maximum value obtained is 160°.

B. Accurate design of the excitation coefficients

The design concept of the feed lines is illustrated in Fig. 6. Regarding the previous example, the radiation elements and feed lines are formed on a single plate in a 4 × 4 array antenna [9]. The objective of this configuration is to design a low-loss feeding network. The presence of a single feed point and the conformation of the series feed network within the column arrays are effective in reducing the feed network losses. Moreover, the conformation of the radiation elements and feed lines on a single plate allows for easy fabrication. The patch antennas and feed lines are formed on a Teflon substrate having electric constants of ε_r = 2.6 and tanδ = 0.0018 and a thickness of 0.8 mm. The frequency in this case is selected as 11 GHz, by considering the use of broadcasting satellite (11 GHz to 12 GHz). Then, the patch size is 8 mm^2. The λ/2 patch separation is 13.6 mm. In this configuration, the design of a four-port power divider at the feed point and the series feed network is sensitive for feed line parameters. Accurate feed line design is performed through try and error process by an electromagnetic simulator.

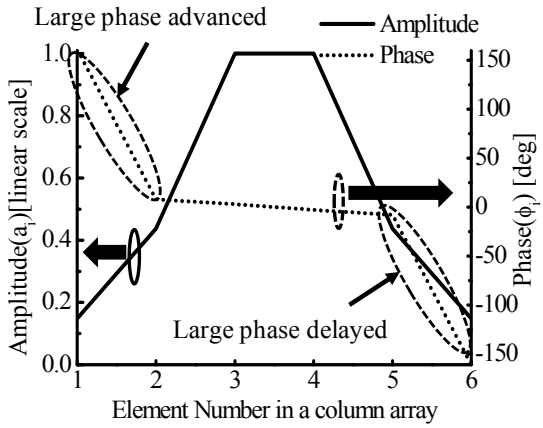

Fig. 5. Excitation coefficients of the feed array.

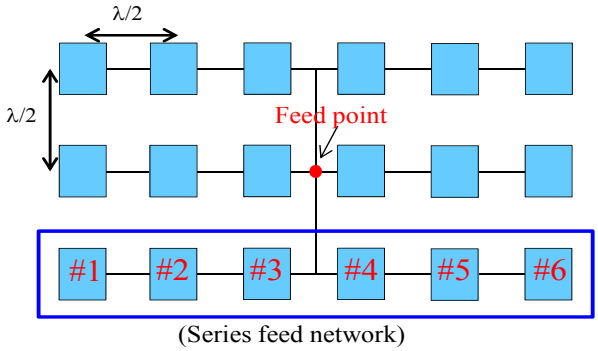

Fig. 6. Design concept of the feed lines.

The actual series feed configuration is shown in Fig. 7. The phase distribution in Fig. 5 is achieved by adjusting the feed line length. At the

line length between P_1 and P_2, a very large phase lead is required. For this, the feed line length has to be very short when compared with the patch spacing. Therefore, a line length of one wavelength is added. The amplitude distribution is achieved by obtaining the appropriate power ratios at the power dividers. As shown in Fig. 7, D_3 denotes the power divider, and P_1 through P_6 denote the power ratios in Fig. 5. Z_T denotes the terminal resistance corresponding to the edge impedance of the patch antenna, and it is set to 127 Ω. Although the patch antennas should be attached to the terminal points, they are replaced by Z_T for design convenience. At the final stage shown in Fig. 12, the patch antennas are attached to the terminals, and certain corrections are mainly added to the line lengths. Z_0 denotes the common feeder line impedance, and it is set to 100 Ω. Z_i denotes the feeder line impedance. Z_A is used to equally divide the source power to the half branches of the array antenna.

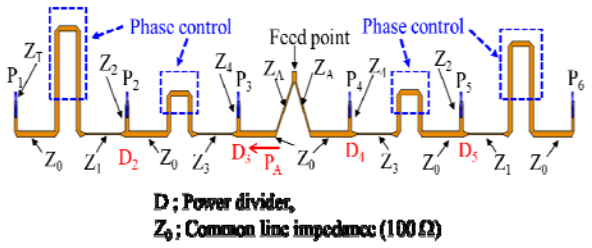

Fig. 7. Series feed configuration.

The fundamental design of a power divider (D_3) is performed on the basis of the following equation,

$$\sqrt{P_A} : \sqrt{P_1 + P_2} = \frac{1}{Z_0} : \frac{1}{Z_3} \tag{4}$$

where P_A is the sum of P_1, P_2, and P_3. The relation of P_1:P_2:P_3 = 0.02:0.19:1.0 is determined from the amplitude relation in Fig. 5. The remaining power dividers, namely, D_2, D_4, and D_5, are designed in a similar manner. The calculated results of all the line impedances are shown in Fig. 8. The values of P_1 and P_6 are very small because Z_1 is very large. The amplitudes and phases of the terminal currents are shown in Fig. 9. These values correspond to the excitation coefficients. The obtained amplitudes and phases of the configuration in Fig. 7 agree very well with the objective values.

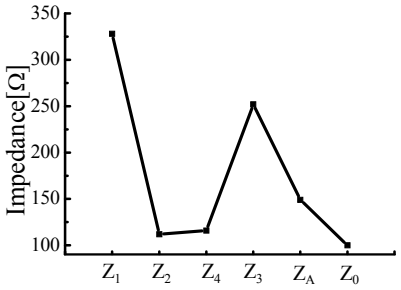

Fig. 8. Impedance.

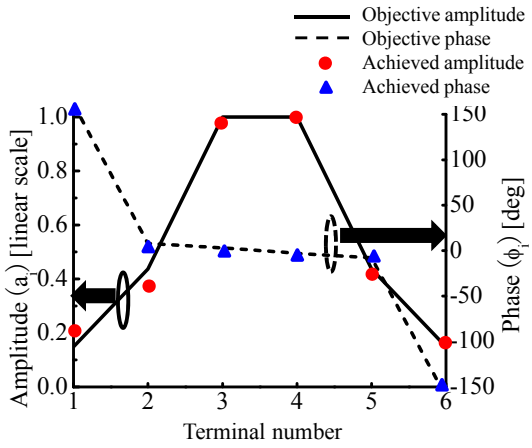

Fig. 9. Terminal currents.

Further, the feed line configuration between the column arrays is shown in Fig. 10. The feed lines to the six central patches are considered for design easiness. In order to achieve the same excitation phase in the column arrays, the feed line lengths are adjusted at the phase control sections. Similar amplitude excitations of the three column arrays are designed at the power divider. At the power divider, a power ratio of P_1:P_2:P_3:P_4 = 2:1:1:2 is obtained by taking into account the same amplitude in the three column arrays. Modifications of the line impedances Z_B and Z_C are required because the line configuration around the power divider is rather complicated. As a result, Z_B = 128 Ω and Z_C = 109 Ω are obtained. In order to ensure the design results, the terminal currents in Fig. 10 are redrawn in Fig. 11. The same magnitudes and phases are realized between the column arrays.

C. Array feed characteristic

The final array feed configuration is shown in Fig. 12. Patch antennas are added to the feed-line

network design, as shown in Figs. 7 and 10. The current amplitudes are shown. Almost the same amplitudes are achieved in the three column arrays.

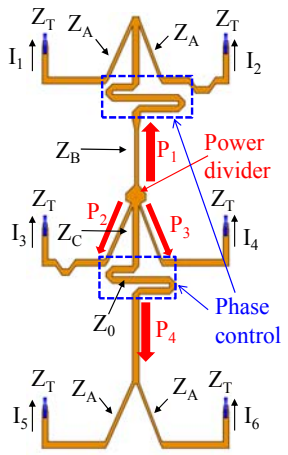

Fig. 10. Feed line design between the columns.

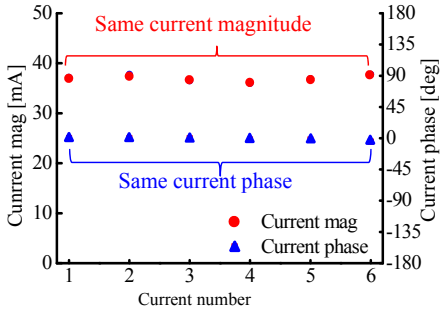

Fig. 11. Terminal currents.

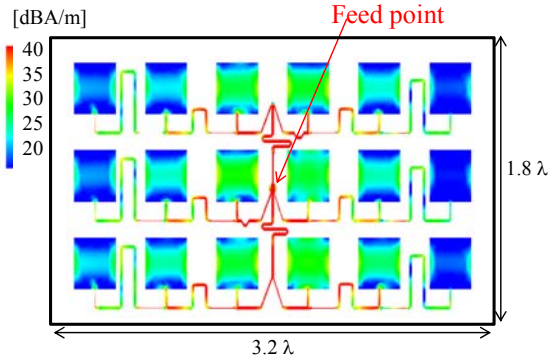

Fig. 12. Array feed configuration.

The excitation coefficients obtained for the patch antennas are shown in Fig. 13. The deviations in the amplitudes and phases between the column arrays are rather small. Excellent excitation coefficients are obtained in the array feed.

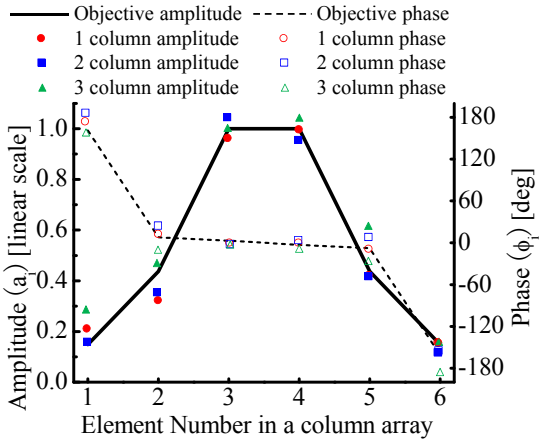

Fig. 13. Excitation coefficient.

In order to measure the realized electrical characteristics, an array feed is fabricated as shown in Fig. 14. Patch antennas and feed lines are fabricated by using a cutting machine. Almost the same shape is achieved as shown in Fig. 12. First, the return loss less than -10 dB is obtained in 9.5 GHz to 10.5 GHz. The center frequency shift from the calculated frequency (11 GHz) is due to the difference of the dielectric constant.

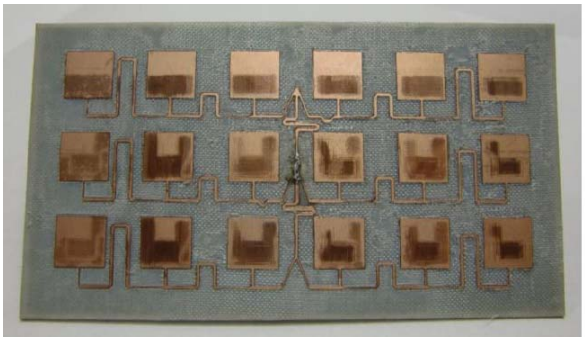

Fig. 14. Fabricated array feed

The radiation patterns of the array feed are shown in Fig. 15. The z_f-x_f plane is shown in Fig. 15 (a). The measured and calculated results agree very well with each other. The maximum electric field level is 12.2 dBi. In order to estimate the feeder loss, the conductivity of the metal is set to infinity, and tanδ of the dielectric substrate is set to zero in the calculations. Then, the feeder loss is estimated to be 0.2 dB. Through this agreement, accurate excitation coefficients are ensured. The z_f-y_f plane is shown in Fig. 15 (b). The measured pattern is broader than the calculated one. This

pattern degradation is due to the slight phase difference between the column arrays.

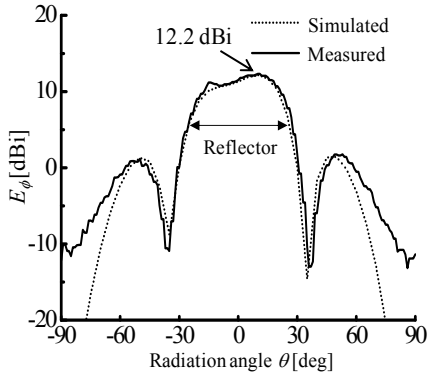

(a) z_f-x_f plane.

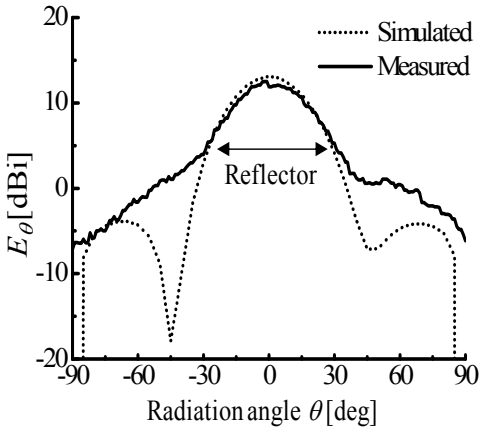

(b) z_f-y_f plane.

Fig. 15. Radiation pattern of the array feed.

III. CHARACTERISTICS OF THE FABRICAED ANTENNA

The fabricated array feed is combined with the fabricated offset parabolic reflector, as shown in Fig. 16 [10]. The reflector is composed of a carbon FRP material. The array feed functions in the horizontal polarization. The radiation angles are denoted as θ and ϕ. The main beam direction is along the x axis, which corresponds to $\theta = 90°$. First, electromagnetic simulations are performed. The simulation parameters are listed in Table I. Although the antenna diameter is only 9.1 times the wavelength, rather large calculation resources are required. The electric near-field distributions are shown in Fig. 17. The radiated electric fields from the array feed are well-concentrated in the reflector region. Regarding the reflected electric fields from the reflector, the electric field intensity for a plane wave is almost constant over the aperture plane.

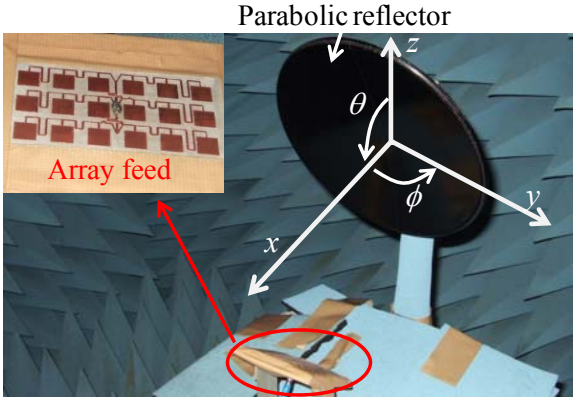

Fig. 16. Fabricated OPA.

The effect of radiation pattern synthesis is ensured through the uniform intensity of the plane wave. At the upper and lower edges of the reflector, appreciable spillover levels are observed.

Table I: Simulation parameters.

Computer	Memory	16 GB
	Clock time	3.2 GHz
Simulator	FEKO Suite 6.0	MoM
Frequency		11 GHz
Antenna diameter		248 mm
Focal length		218 mm
Mesh size		0.02 mm (array feed) 8.30 mm (reflector)
Number of meshes		15498
Simulation memory		7.9 GB
Simulation time		6.9 hours

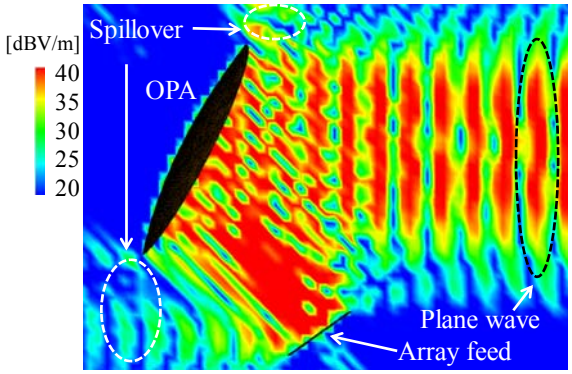

Fig. 17. Electric near-field distribution.

Finally, the measured radiation characteristics are compared with the calculated results. The wide-angle radiation patterns are shown in Fig. 18. In the *x-y* plane shown in Fig. 18 (a), the measured results for the main beam shape is in good agreement with the calculated results. In the *x-z* plane shown in Fig. 18 (b), the measured results for the main beam and side lobes are in good agreement with the calculated results. In particular, appreciable spillovers are observed in the zenith direction ($\theta = 0°$) and reflector backward direction ($\theta = 90°$).

The near-axis radiation patterns are shown in Fig. 19. In the *x-y* plane shown in Fig. 19 (a), the measured antenna gain of 26.0 dBi is only 0.4 dB lower than the calculated results. The measured side lobes are larger than the calculated levels by more than 5 dB. These increases correspond to the radiation pattern distortion shown in Fig. 15 (b). In the *z-x* plane shown in Fig. 19 (b), the measured and calculated results agree very well with each other. Excellent radiation pattern synthesis in this plane is ensured. In order to estimate the aperture efficiency, the antenna loss budgets are summarized in Table II. For uniform aperture distribution, the actual antenna gain is 26.8 dBi taking into account the losses. Further, the measured gain of 26.0 dBi corresponds to 83.2 % antenna aperture efficiency. High aperture efficiency is ensured.

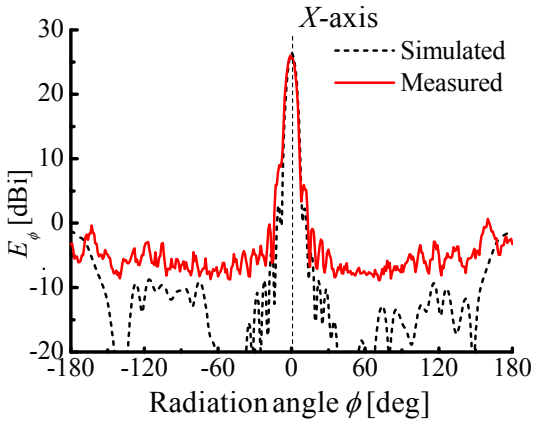

(a) *x-y* plane.

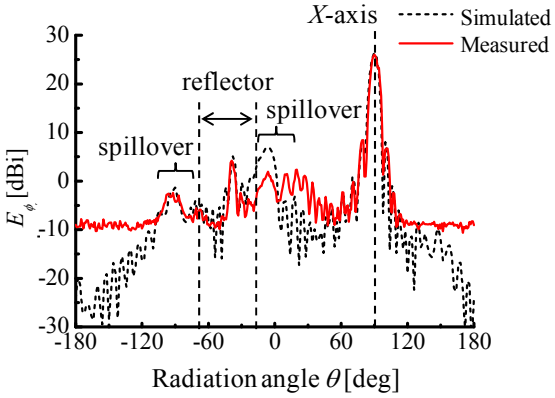

(b) *z-x* plane.

Fig. 18. Wide-angle radiation pattern.

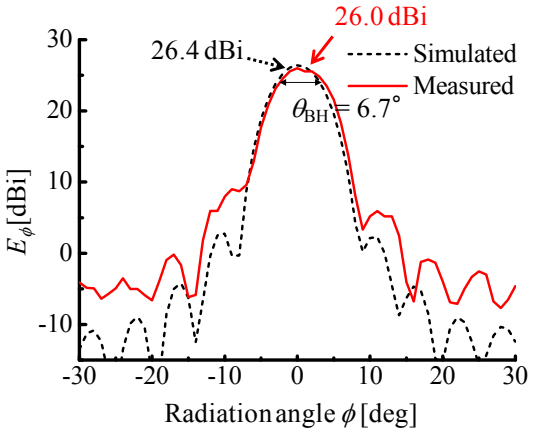

(a) *x-y* plane.

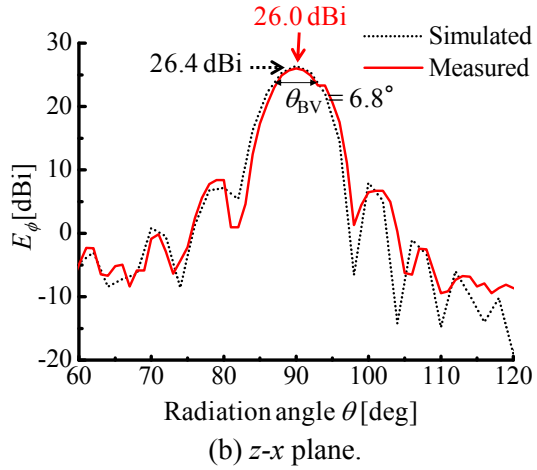

(b) *z-x* plane.

Fig. 19. Near-axis radiation pattern.

Table II: Antenna loss budgets.

		Gain	Aperture Efficiency (η_{ap})
Uniform aperture distribution		28.2 dBi	100%
Losses	Spill over	1.2 dB	
	Feed loss	0.2 dB	
Actual gain		26.8 dBi	100%
Measured gain		26.0 dBi	83.2%

IV. CONCLUSION

Radiation pattern synthesis of an array feed is performed in order to achieve uniform aperture illumination for the offset antenna. The design of the important excitation coefficients of the array feed is successfully performed through accurate electromagnetic simulations. The design accuracies are ensured through the measured results of the fabricated array feed. Moreover, the antenna radiation characteristics are obtained by combining the array feed with a parabolic reflector. An increased antenna aperture efficiency of 83.2% is ensured from the measured antenna gain.

REFERENCES

[1] K. Miwa, M. Tanaka, T. Naito, and Y. Endo, "A new FRP parabolic antenna for satellite broadcasting system," *ITE Technical Report*, vol. 8, no. 7, pp. 7-12, May 1984.

[2] http://www42.tok2.com/home/fleet7/FilmScanner/NegaScanJGSDFe.html, Antennas of TASCOM －X.

[3] A. Rudge and N. Adatia, "Offset-parabolic-reflector antennas: A review," *Proc. IEEE*, vol. 66, pp. 1592-1618, 1978.

[4] C. Han, "A multifeed offset reflector antenna for the Intelsat V communication satellite," *Proc. 7th European Microwave Conf.*, pp. 343-347, 1977.

[5] S. Lee and Y. Samii, "Simple formulas for designing an offset multibeam parabolic reflector," *IEEE Trans. Antennas and Propag.*, vol. 29, no. 3, pp. 472-478, 1981.

[6] J. Huang and Y. Samii, "Fan beam generated by a linear-array fed parabolic reflector," *IEEE Trans. Antennas and Propag.*, vol. 38, no. 7, pp. 1046-1052,1990.

[7] Y. Samii, J. Huang, B. Lopez, M. Lou, E. Im, S. Durden, and K. Bahadori, "Advanced precipitation radar antenna: Array-fed offset membrane cylindrical reflector antenna," *IEEE Trans. Antennas and Propag.*, vol. 53, no. 8, pp. 2503-2515, 2005.

[8] J. Shinohara, Y. Yamada, N. Michishita, M. Islam, and N. Misran, "Design of an array feed offset parabolic reflector antenna used for a simple earth station," *Int. Conf. Space Science and Commun.*, Paper ID 81, 2011.

[9] A. Mallahzadeh and M. Taherzadeh, "Investigation of a proposed ANN-based array antenna diagnosis technique on a planar microstrip array antenna," *ACES Journal*, vol. 26, no. 8, pp. 667-678, Aug. 2011.

[10] J. Shinohara, N. Michishita, Y. Yamada, M. Islam, and N. Misran, "Measured electrical characteristics of an array feed offset parabolic reflector antenna," ISAP'12, POS2-19, pp. 1104-1107, 2012.

Naobumi Michishita received his B.E., M.E., and D.E. degrees in Electrical and Computer Engineering from Yokohama National University in 1999, 2001, and 2004, respectively. In 2004, he joined the Department of Electrical and Electronic Engineering, National Defense Academy, as a research associate. From 2006 to 2007, he was a visiting scholar at the University of California, Los Angeles. In 2004 and 2005, he received the Young Engineer Award from the IEEE AP-S Japan Chapter and IEICE, respectively. His current research interests include metamaterial antennas and electromagnetic analysis. He is a member of IEEE.

Junichi Shinohara graduated from the Department of Electronic Engineering, National Defense Academy, in 2008. He belongs to the Japan Ground Self-Defense Force. He completed his master's program in engineering at the National Defense Academy in 2013. He has been engaged in research on parabolic reflector antennas. He is now an instructor in the JGSDF signal school as a Second Lieutenant.

Yoshihide Yamada graduated from the Nagoya Institute of Technology and received his BS and MS degrees in electronics in 1971 and 1973, respectively. In 1989, he received his DE degree from the Tokyo Institute of Technology. In 1973, he joined the Electrical Communication Laboratories at the Nippon Telegraph and Telephone Corporation (NTT). Until

1984, he was engaged in research and development (R&D) related to reflector antennas for terrestrial and satellite communications. Beginning in 1985, he engaged in R&D for base station antennas for mobile radio systems. In 1993, he moved to NTT Mobile Communications Network Inc. (NTT DoCoMo). In 1995, he was temporarily transferred to YRP Mobile Telecommunications Key Technology Research Laboratories Co., Ltd. In 1996, he was a guest professor at the Cooperative Research Center at Niigata University as well as a lecturer at the Science University of Tokyo. In 1998, he took a position as a professor at the National Defense Academy. His current research interests include very-small normal-mode helical antennas, reflector antennas, and radar cross sections.

He is a fellow member of IEICE; a member of JSST of Japan; a member of ACES; and a senior member of IEEE AP, VT, and COMM.

Mohammad Tariqul Islam received his B.Sc. and M.Sc. degrees in Applied Physics and Electronics in 1998 and 2000, respectively, from the University of Dhaka, Dhaka, Bangladesh and a Ph.D degree in telecommunication engineering from the Universiti Kebangsaan Malaysia (UKM) in 2006. He is currently a professor at the Institute of Space Science (ANGKASA), UKM, Malaysia. He has been very promising as a researcher and a recipient of several international gold medals, the Best Invention in Telecommunication award, and a special award from Vietnam for his research and innovation. He has filed six patent applications. He has authored and co-authored 102 international journal papers, 90 international and local conference papers, and 3 books. Thus far, his publications have been cited 560 times, and the H-index is 15 (Source: Scopus). He has been awarded “Best Researcher Award” in 2010 and 2011 at UKM. He served as a faculty member at the Multimedia University (MMU), Malaysia, from May 2007 until May 2008. His research interests concern enabling technology for RF, antenna technology, electromagnetic absorption, and radio astronomy instruments. He is currently handling many research projects from the Ministry of Science, Technology, and Innovation (MOSTI) and the Ministry of Higher Education, Malaysia (MOHE).

Norbahiah Misran received her B.Eng. degree in Electrical, Electronic, and System Engineering from Universiti Kebangsaan Malaysia in 1999. She completed her Ph.D. degree in Communication Engineering at the Queen’s University of Belfast, United Kingdom, in 2004. She started her career as a tutor at the Department of Electrical, Electronic, and System Engineering, Universiti Kebangsaan Malaysia in 1999. She has been as a lecturer since 2004 and was appointed as an associate professor in 2009. Since 2012, she has been a professor at Universiti Kebangsaan Malaysia as well as an associate senior research fellow at the Institute of Space Science, Universiti Kebangsaan Malaysia. Her current research interests include RF device design, particularly microstrip antenna technology, and reflect array antennas. She is also involved in engineering education research.